long arm of the X chromosome are so small that they can be detected only in late prophases (Fig. 2). Previously, the small chimpanzee Y chromosome was reported as indistinctly banded (*1, 9*). In this work, however, we found a banding pattern similar to that in man, except with less heterochromatin at the distal end of the long arm and more around the centromere (Figs. 1 and 2). Significant differences in the number and thickness of various bands on several chromosomes (4, 6, and 16) were shown in the comparative diagrams of the Paris report (*3*). These differences could not be confirmed in our detailed analysis of these chromosomes at various stages of condensation.

As a result of this and previous work, it has become evident that the chromosomal differences between man and chimpanzee are largely confined to the existence of nine pericentric inversions, addition of telomeric heterochromatin in 18 chimpanzee chromosomes (Fig. 2), and differences in amount of pericentromeric, paracentromeric, intercalated, and Y-type heterochromatin. The various types of constitutive heterochromatin are known to be enriched in nontranscribed highly repeated DNA sequences (*5*), and pericentric inversions have not been shown to produce changes in gene expression; therefore, the differences observed at the chromosomal level between man and chimpanzee appear to be of no consequence to their phenotype.

The virtual homology of the nonheterochromatic bands of man and chimpanzee is not surprising because more than 20 genes have been localized to homologous chromosomes and chromosome bands of the two species (*10*), the amino acid sequence of a large number of proteins studied in the two species is similar (*11*), and there is a large degree of homology of repeated and unique copy DNA in both species (*12*). Previous reports have also cited the finding of a chimpanzee with the clinical, behavioral, and cytogenetic features of Down's syndrome (*13*). Such a remarkable degree of similarity makes difficult a precise explanation of the large biological differences observed between these two closely related species.

JORGE J. YUNIS*
JEFFREY R. SAWYER
Department of Laboratory Medicine and Pathology, University of Minnesota Medical School, Minneapolis 55455
KELLY DUNHAM
Department of Preventive Medicine, University of Iowa, Oakdale 52319

References and Notes

1. C. C. Lin, B. Chiarelli, L. E. M. de Boer, M. M. Cohen, *J. Hum. Evol.* **2**, 311 (1973); J. de Grouchy, C. Turleau, M. Roubin, M. Klein, *Ann. Genet.* **15**, 79 (1972); P. Pearson, *Nobel Symp.* **23**, 145 (1973); J. Lejeune, B. Dutrillaux, M.-O. Rethoré, M. Prieur, *Chromosoma* **43**, 423 (1973).
2. B. Dutrillaux, "Sur la nature et l'origine des chromosomes humains," *Monogr. Ann. Genet. Expansion Sci. Fr.* (1975), pp. 41-71.
3. Paris Conference (1971), supplement (1975); "Standardization in human cytogenetics," *Cytogenet. Cell Genet.* **15**, 201 (1975).
4. A pericentric inversion represents an inversion of a chromosome segment that involves the centromere and has a breakpoint in each chromosome arm.
5. Constitutive heterochromatin represents chromosome material that is highly condensed in the interphase nucleus and is enriched in nontranscribed, highly repeated DNA sequences [J. J. Yunis and W. G. Yasmineh, *Science* **174**, 1200 (1971); K. W. Jones, in *Molecular Structure of Human Chromosomes*, J. J. Yunis, Ed. (Academic Press, New York, 1977), p. 295].
6. J. J. Yunis, J. R. Sawyer, D. W. Ball, *Chromosoma* **67**, 293 (1978); J. J. Yunis, D. W. Ball, J. R. Sawyer, *Hum. Genet.* **49**, 291 (1979).
7. J. J. Yunis, L. Roldan, W. G. Yasmineh, J. C. Lee, *Nature (London)* **231**, 532 (1971); M. E. Chandler and J. J. Yunis, *Cytogenet. Cell Genet.* **22**, 352 (1979).
8. Dutrillaux (*2*) considers the fusion as telomeric and interprets the terminal heterochromatin seen in the two chimpanzee acrocentric chromosomes to have arisen after the divergence of the two species.
9. D. A. Miller, *Science* **198**, 1116 (1977).
10. P. L. Pearson, in *Molecular Structure of Human Chromosomes*, J. J. Yunis, Ed. (Academic Press, New York, 1977), p. 267.
11. M.-C. King and A. C. Wilson, *Science* **188**, 107 (1975).
12. P. L. Deininger and C. W. Schmid, *ibid.* **194**, 846 (1976).
13. H. M. McClure, K. H. Belden, W. A. Pieper, C. B. Jacobson, *ibid.* **165**, 1010 (1969); F. H. Ruddle and R. P. Creagan, *Annu. Rev. Genet.* **9**, 407 (1975).
14. This research was supported by NIH grant GM26800 (to J.J.Y).
* Correspondence should be addressed to J.J.Y.

3 December 1979

Oxygen Consumption and Cellular Ion Transport: Evidence for Adenosine Triphosphate to O_2 Ratio Near 6 in Intact Cell

Abstract. *Oxygen (O_2) consumption and net K^+ uptake were measured simultaneously upon reintroduction of K^+ into a K^+-depleted suspension of renal tubules. The K^+/O_2 stoichiometries of 11.8 ± 0.2 and 8.4 ± 0.6 were obtained for reduced nicotinamide adenine dinucleotide- and flavoprotein-linked substrates, respectively. These values complement classical K^+ to adenosine triphosphate (ATP) and ATP/O_2 stoichiometries, thereby demonstrating a remarkably efficient coupling between the processes of Na^+- and K^+-dependent adenosinetriphosphatase-mediated ion transport and oxidative phosphorylation within the intact cell.*

Potassium uptake and sodium extrusion by mammalian epithelial cells are dependent on oxidative metabolism and Na^+- and K^+-dependent adenosinetriphosphatase (ATPase)-mediated ion transport. Individually, the production of adenosine triphosphate (ATP) by way of oxidative phosphorylation and the hydrolysis of ATP by the Na^+,K^+-ATPase have been well documented (*1-3*). However, the scheme by which these two fundamental processes work in concert within the intact cell has not been entirely defined. Measurements of renal cell adenine nucleotide levels by Balaban *et al.* (*4*) lend experimental support to the contention (*5*) that the generation of adenosine diphosphate (ADP) by the Na^+,K^+-ATPase is instrumental in providing the signal for synchronous oxidative metabolism. These measurements suggest that the processes of transport and oxidative phosphorylation are coupled within the intact cell via their

Table 1. The K^+/O_2 ratio for potassium uptake in K^+-depleted renal tubules. The K^+/O_2 ratios were calculated on the basis of individual experiments as illustrated in Fig. 1A. Average values for the absolute rates of QO_2 and K^+ uptake are provided for the purposes of comparison between the substrates. Succinate-supplemented cells were prepared by using a modified K^+-free suspension medium containing NaCl (100 m*M*), $NaHCO_3$ (25 m*M*), NaH_2PO_4 (4 m*M*), $CaCl_2$ (2.3 m*M*), $MgSO_4$ (2.0 m*M*), Na_2-succinate (20 m*M*), glucose (5 m*M*), and dextran (molecular weight, 40,000; 0.6 percent). The temperature was 37°C and the *p*H 7.4. Protein concentrations were in the range of 4 to 10 mg/ml. Values are given as means ± standard error.

Substrate	Experiments (No.)	K^+/O_2	QO_2 (nmole O_2/min-mg protein)		K^+ uptake immediately after KCl addition (nmole K^+/min-mg protein)
			Prior to KCl addition	KCl addition	
Glucose + lactate + alanine	16	11.8 ± 0.2	11 ± 1	20 ± 1	103 ± 7
Succinate + glucose	4	8.4 ± 0.6	29 ± 4	42 ± 6	112 ± 30

0036-8075/80/0606-1148$00.50/0

common intermediaries—the cellular ADP and ATP pools. To further explore the relation between transport and oxidative metabolism within the intact cell we have determined a stoichiometry for the incremental oxygen consumption associated with ouabain-inhibitable potassium uptake (K^+/O_2 ratio). The K^+/O_2 value of 11.8 obtained in this study of renal cortical tubules indicates an extremely tight coupling between Na^+,K^+-ATPase-mediated ion transport (K^+/ATP = 2) and reduced nicotinamide adenine dinucleotide (NADH)-linked oxidative phosphorylation (ATP/O_2 = 6). These findings demonstrate that the mitochondrial phosphorylating mechanism is able to meet the ATP demands of cellular ion transport with a remarkably high degree of efficiency.

Figure 1A illustrates the simultaneous traces obtained from a potassium ion selective electrode (K^+/Na^+ selectivity > 1000) and a Clark-type oxygen electrode upon injection of a KCl bolus into a K^+-depleted suspension of isolated renal tubules respiring on glucose, lactate, alanine, and endogenous substrate. The upper portion of the figure indicates that the K^+ concentration of the medium is 0.46 m*M* prior to the KCl injection and that the injection initially raises the K^+ concentration above 2 m*M*. The lower half of Fig. 1A shows that a biphasic increase in the rate of O_2 consumption (QO_2) occurs after the injection. The first phase of increased QO_2 is temporally correlated with a rapid semilogarithmic period of K^+ uptake, whereas the second and slower phase coincides with a reduction in the rate of net K^+ uptake. The system approaches a new steady state characterized by a faster QO_2 and a higher medium K^+ concentration than were present prior to the KCl addition. A second KCl bolus added to the suspension in Fig. 1A is unable to elicit the response seen in the fully K^+-depleted tubules and, as anoxia is reached, K^+ leaks out of the tubules as would be expected in the case of aerobically supported ion transport.

The synchrony between the rapid initial periods of K^+ uptake and incremental O_2 consumption makes it convenient to consider this phase of the recording as an initial rate period. The first 10 seconds following the KCl injection are excluded in our measurements of the initial rate period since this time was required to achieve a stable K^+ electrode trace. Optical measurements of NADH fluorescence and biochemical measurements of the cellular ATP and ADP pools performed under identical conditions (*4*) demonstrate that the K^+ uptake measured during the initial rate period does not reflect the depletion of an endogenous ATP pool but rather depends directly on a new level of increased aerobic metabolism initiated by the KCl addition. Dividing the K^+ uptake by the incremental O_2 consumption for the designated initial rate period yields a K^+/O_2 ratio of 11.7 for the trace in Fig. 1A. As shown in Table 1, the results of 16 such experiments yield an average K^+/O_2 ratio of 11.8 ± 0.2 (range 10.0 to 12.9). Although technically it is known that the K^+ electrode monitors net uptake, it is

Table 2. Oxidative phosphorylation in renal cortical mitochondria at 37°C. Mitochondria were prepared in sucrose medium by a standard centrifugation technique after Nagarse protease treatment of the tissue mince. The assay medium, *p*H 7.4, consisted of KCl (115 m*M*), KH_2PO_4 (5 m*M*), K^+-containing 4-(2-hydroxyethyl)-1-piperazineethanesulfonate buffer (10 m*M*), and substrate to which an appropriate portion of mitochondrial concentrate was added giving a final protein concentration of 2 mg/ml. Final substrate concentrations when present were glutamate, 6.0 m*M*; malate, 6.2 m*M*; and succinate, 5.1 m*M*. Respiratory control ratios at 37°C for glutamate- and malate-supported respiration were in the range of 5 to 6, whereas those for succinate-suported respiration were in the range of 3 to 4.

Substrate	ADP/O	ADP/ΔO
Glutamate + malate	2.23 ± 0.07	2.79 ± 0.08
Glutamate + malate + ouabain (60 μ*M*)	2.18 ± 0.07	2.76 ± 0.10
Succinate + Mg^{2+}*	1.59 ± 0.01	2.23 ± 0.01
Succinate + Mg^{2+}* + rotenone (9 μ*M*)	1.43 ± 0.03	1.99 ± 0.07
Succinate + malate + glutamate	1.45 ± 0.05	2.07 ± 0.06

*1 m*M*.

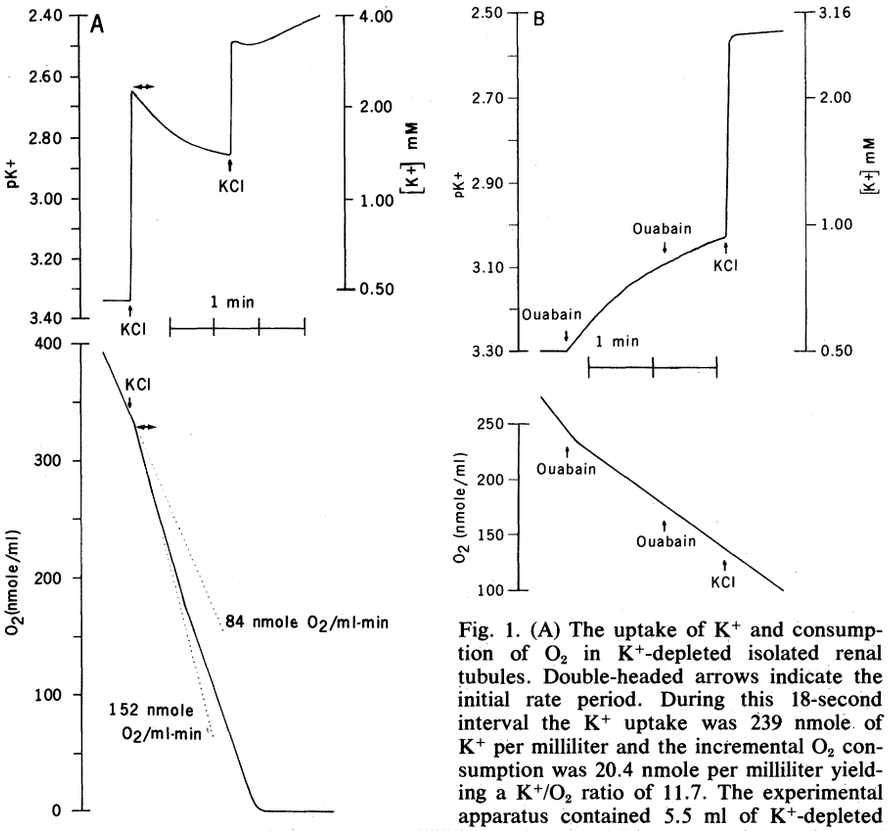

Fig. 1. (A) The uptake of K^+ and consumption of O_2 in K^+-depleted isolated renal tubules. Double-headed arrows indicate the initial rate period. During this 18-second interval the K^+ uptake was 239 nmole of K^+ per milliliter and the incremental O_2 consumption was 20.4 nmole per milliliter yielding a K^+/O_2 ratio of 11.7. The experimental apparatus contained 5.5 ml of K^+-depleted tubule suspension (9 mg of protein per milliliter) and KCl additions were in the form of 10-μl portions of a stock of 1*M* KCl solution. (B) The release of K^+ and consumption of O_2 in ouabain-treated K^+-depleted tubules. The chamber contained 8.5 ml of K^+-depleted suspension and the KCl injection consisted of 15 μl of a stock of 1*M* KCl. Ouabain was added in the form of two 25 μl-portions of a 0.010*M* stock solution to give a final concentration of 60 μ*M*. The rabbit kidney cortical tubules were prepared as previously described (*9*) and K^+ depletion was achieved by washing the suspension three times in K^+-free Ringer of the composition NaCl (115 m*M*), $NaHCO_3$ (25 m*M*), NaH_2PO_4 (4 m*M*), $CaCl_2$ (2.3 m*M*), $MgSO_4$ (2.0 m*M*), glucose (5 m*M*), lactate (4 m*M*), alanine (1 m*M*), and dextran (molecular weight, 40,000; 0.6 percent). The experimental apparatus was of the type previously described (*9*) except for modifications related to the outfitting of a K^+-sensitive electrode (Orion Corp.) and Ag/AgCl reference. Electrode calibrations were performed prior to and following each experiment in order to restrict to the 10 percent level possible errors in accuracy due to electrode drift. All experiments were performed at 37°C and *p*H 7.4.

probable that the measurements of K^+ utilized in calculating the K^+/O_2 ratio represent primarily increments in the influx of K^+, because it is unlikely that efflux is significantly altered during the brief initial rate period. Protein concentrations varied over a range of 4 to 10 mg of protein per milliliter but had no discernible effect on the K^+/O_2 ratio.

The rapid initial phase of K^+ uptake is mediated by a K^+-induced stimulation of the ouabain-sensitive Na^+,K^+-ATPase. This is consistent with the observation that the medium K^+ concentration prior to injection is well below reported K_m values (Michaelis constant) for the ouabain-sensitive Na^+,K^+-ATPase in the presence of 150 m*M* sodium (*3*). Figure 1B illustrates the total inhibition of K^+ uptake induced by the prior addition of 60 μM ouabain. In fact, immediately after ouabain administration to K^+-depleted tubules there is a decrease in respiration and an efflux of K^+, indicating the inhibition of extant Na^+,K^+-ATPase activity by the glycoside.

The effect of 20 m*M* succinate supplementation on the K^+/O_2 ratio was examined because flavoprotein-linked substrates are expected to produce fewer ATP molecules per O_2 consumed. The average K^+/O_2 ratio obtained with succinate was 8.4 ± 0.6 (range 6.7 to 9.5, see Table 1). This value is consistent with the observation in isolated mitochondria that flavoprotein-linked respiration proceeds with two-thirds of the ATP-producing capacity of NADH-linked respiration. The possibility of a significant contribution from NADH-linked respiration was not precluded in these experiments since rotenone was not present. However, experiments with isolated mitochondria shown in Table 2 indicate that the efficiency of oxidative phosphorylation for succinate alone or in combination with NADH-linked substrates approximates that of succinate and rotenone.

The mitochondrial phosphorylation ratios presented in Table 2 demonstrate that the rabbit renal cortex possesses an orthodox phosphorylation system and that the effect of ouabain on the renal tubules is not the result of mitochondrial toxicity. The ratios were obtained by the polarographic technique (*2*) and values were calculated by using both the total oxygen excursion (ADP/O) and the incremental oxygen excursion (ADP/ΔO) observed during an ADP-induced period of state 3 respiration. This distinction is noteworthy (*1*, *6*) because the K^+/O_2 ratio calculated for K^+ transport in the intact tubules is based on incremental oxygen consumption. The phosphorylation ratios obtained are in excellent agreement with those reported by Hinkle and Yu (*1*) for NADH-linked (glutamate and malate) and succinate-supported respiration in rat liver mitochondria. Earlier observations (*7*, *8*) indicating that ouabain has no direct effect on the rate of mitochondrial respiration were also confirmed (not shown).

The K^+/O_2 ratio of 11.8 ± 0.2 obtained in this study indicates that an extremely efficient coupling exists between Na^+,K^+-ATPase-mediated ion transport ($K^+/ATP = 2$) and NADH-linked oxidative phosphorylation ($ATP/O_2 = 6$) within the intact cell. This value is appreciably higher than the K^+/O_2 ratio of 4 obtained by Whittam and Willis (*5*) for kidney cortex slices and reflects both the rapid kinetic capability and superior oxygenation characteristics (*9*) of our experimental preparation. A review of the literature indicates that K^+/ATP ratios determined in three different red cell preparations (*10*–*12*) yielded values somewhat higher than 2 (2.2 to 2.4), whereas the results of experiments in a reconstituted renal ATPase preparation (*13*) lacked sufficient resolution to discriminate between integral and fractional values. In view of some uncertainty within the literature regarding the precise evaluation of K^+/ATP and ADP/O coupling ratios, we propose that the 11.8 ± 0.2 value be not strictly viewed as the product of 2 and 6; rather it may be indicative of numbers 10 to 20 percent greater than 2 and 10 to 20 percent less than 6, respectively. We conclude that the excellent correlation between phosphorylation ratios and K^+/O_2 ratios for both NADH-linked and succinate-supplemented respiration indicates that in vitro mitochondrial studies are indeed valid indices of energy metabolism within the intact cell.

STUART I. HARRIS
ROBERT S. BALABAN*
LAZARO J. MANDEL
Department of Physiology,
Duke University Medical Center,
Durham, North Carolina 27710

References and Notes

1. P. C. Hinkle and M. L. Yu, *J. Biol. Chem.* **254**, 2450 (1979).
2. B. Chance and G. R. Williams, *ibid.* **217**, 383 (1955).
3. A. Schwartz, G. E. Lindenmayer, J. C. Allen, *Pharmacol. Rev.* **27**, 3 (1975).
4. R. S. Balaban *et al.*, *Proc. Natl. Acad. Sci. U.S.A.* **77**, 447 (1980).
5. R. Whittam and J. S. Willis, *J. Physiol. (London)* **168**, 158 (1963).
6. J. E. Davis, L. Lumeng, D. Bottoms, *FEBS Lett.* **39**, 9 (1974).
7. R. S. Balaban and L. J. Mandel, *J. Physiol. (London)*, in press.
8. D. M. Blond and R. Whittam, *Biochem. J.* **92**, 158 (1974).
9. R. S. Balaban, S. P. Soltoff, J. M. Storey, L. J. Mandel, *Am. J. Physiol.* **238**, F50 (1980).
10. P. J. Garrahan and I. M. Glynn, *J. Physiol. (London)* **192**, 217 (1967).
11. R. Whittam and M. E. Ager, *Biochem. J.* **97**, 214 (1965).
12. A. K. Sen and R. L. Post, *J. Biol. Chem.* **239**, 345 (1964).
13. S. M. Goldin, *ibid.* **252**, 5630 (1977).
14. This work was supported by the Walker P. Inman Fund of Duke University Medical Center and by NIH grants GM-07171 and GM-00929.
* Present address: University of Oxford, Nuffield Department of Clinical Biochemistry, Radcliffe Infirmary, Oxford OX2 6HE, England.

8 November 1979; revised 29 January 1980

Intercellular Adhesion: Coconstruction of Contractile Heart Tissue by Cells of Different Species

Abstract. *Dissociated embryonic rat myocardial cells and chick myocardial cells labeled with radioactive isotope coaggregate and establish intercellular junctions. These bispecific cells reconstruct synchronously beating myocardial tissue within 24 hours of culture.*

By conducting experiments with dissociated embryonic cells and observing the subsequent aggregation of the cells and tissue reconstruction, biologists have been able to learn something about the mechanism of cell movement and organization that leads to the differentiation of tissues in embryos. The dissociated cells from two or more different tissues of the same species segregate according to tissue type (*1*, *2*). This cellular process is widely regarded as a form of histotypic self-recognition. One way to understand histotypic recognition is to examine its operation among different animal species. Moscona and his collaborators (*3*, *4*) studied aggregates containing mouse and chick embryonic cells derived from the same type of tissue. They used embryonic limb precartilage, liver, skin, neural retina, and kidney and reported that the mouse and chick cells of the same type did not sort out according to species. From these studies it was hypothesized that, for any one embryonic cell type, the properties responsible for cell sorting were indistinguishable among even very distantly related warm-blooded vertebrate species. Later, Burdick and Steinberg (*5*), working with the embryonic heart cells from mouse and chick at the light microscopic level, reported that mouse and chick myocardial cells segregated

0036-8075/80/0606-1150$00.50/0